Journal of Russian Laser Research, Volume 18, Number 1, 1997

POLARIZATION ANALYZERS OPERATING IN A WIDE SPECTRAL RANGE

V. A. Zubov

P. N. Lebedev Physical Institute, Russian Academy of Sciences, Leninsky Pr. 53, Moscow 117924, Russia

Abstract

Different versions of practical realization of customary optical systems for full measurement of the polarization state of quasi-monochromatic partially polarized light are considered. They can be used to overcome measurement difficulties associated with the finite width of the spectral range being studied.

The effect of changes in characteristics of optical and polarization elements over a spectral range on the character of polarization measurements is analyzed. Methods for elimination of chromatism or taking into account its effect on measurements are suggested. Relations for taking into account the effect of chromatism of a phase plate with constant thickness on measurement results are given.

Operation of a classical four-channel scheme for studing quasi-monochromatic partially polarized light in the visible and near-IR regions is considered. For this system, expressions are derived which make possible determination of Stokes parameters taking into account the effect of a finite spectral range.

A system using phase modulation of radiation by an electrooptical cell and measurement of the maximum and minimum intensities of the modulated signal is considered. Measurements are carried out by using a two-channel system. Expressions are derived which make possible determination of Stokes parameters for the system under consideration in the visible and near-IR spectral regions.

A system for measuring the polarization state of radiation in the visible and near-IR regions and based on modulation of radiation by an electrooptical phase cell is described. Measurements are carried out for the fundamental modulation frequency and its harmonics using a two-channel scheme. Relations for determining Stokes parameters of the system are presented.

1. Introduction

Polarization, like spectral purity and coherence, is one of the distinguishing features of radiation that frequently requires careful and accurate characterization. The orientation of the electric field of a light wave is of major importance in the radiation-matter interaction problem, because in this case the interaction of electric dipoles of matter with an electric field of a light wave has a dominant role. Polarization analysis is needed for applications of laser radiation, in particular, to interferometry, optical location, holography, and optical communication. Therefore, it is not surprising that the earliest studies of laser characteristics dealt with polarization measurements (see, e.g., [1–3]).

Studies of the polarization of laser radiation include measurements of the polarization state of the incident laser radiation and changes in polarization due to interaction with objects or the enviroment, propagation through communication networks, etc. [4, 5]. If there is a preferred direction in a resonator that is orthogonal to its optical axis or, in other words, the resonator is anisotropic, laser radiation is characterized by a certain degree of polarization. The preferred direction may be specified by the characteristics of the laser active medium or by the resonator construction. Resonator anisotropy may be due to the predetermined position of the crystal axis in solid-state laser media, nonuniformity of pumping, temperature distribution, Brewster windows, and special anisotropic elements that are placed inside the resonator to measure or control the

Translated from a manuscript submitted October 15, 1995.

1071-2836/97/1801-0017$18.00

radiation parameters [6–9]. Preferred polarization, as a rule, is absent when the active material and the resonator have no anisotropic properties. This is observed, in particular, in lasers with high gain, such as metal vapor lasers, neodimium glass lasers, and some semiconductor lasers [10, 11]. The polarization state can be substantially changed by interaction with some object or material or by propagation through optical or fiber-optic communication channels. These changes contain information about these objects, materials, or channels. Methods of polarization studies, such as polarimetry, ellipsometry, and spectropolarimetry [12–18] and the methods used for the study and control of optical communication lines [19], are based on measurements of these changes.

In the literature, several systems have been proposed to measure the polarization state of partially polarized quasi-monochromatic light [19–25]. These systems are generally based on classical approaches to the measurement of polarization. They either measure the intensity in four independent channels with predetermined polarization states [19–21] or use modulation of the analyzed radiation by rotating a polarizer or a phase plate [22–25]. The problems of fabrication of such systems involve expansion of their measuring capabilities. In particular, some problems require that measurements of polarization be carried out in a wide spectral range. Under these conditions, the chromatism of the optical elements used in the system comes into play. This relates also to studies of quasi-monochromatic radiation with a certain coherence time and ultrashort laser pulses. Note that when Δt is the characteristic coherence time or the pulse duration, the spectral width $\Delta\nu$ is determined by the expression $\Delta\nu = 1/\Delta t$ or $|\Delta\lambda| = \lambda^2/(c\Delta t)$. Moreover, the practical incovenience of traditional methods is associated with the use of mechanical devices, which reduce the measurement rate and produce additional noise.

This paper presents a theoretical analysis of three polarization analyzer designs that are based on classical optics. The influence of nonideality of optical elements, specifically, chromatism and finite numerical aperture, on the accuracy of measurement of Stokes parameters is studied. This analysis permits one to select fabrication criteria allowing the polarization analyzer to be used in a wide spectral range.

2. Chromatism of Optical Elements of Polarization Analyzers

The distinctive feature of the measuring systems considered below is the ability to study polarization in a wide spectral range. In this case, a general description must take into account the chromatism of individual optical elements and an analysis of its influence on measurements. A polarization analyzer contains optical elements forming the desired beam structure. Polarization elements are used to separate out a definite linear polarization or change the polarization state in a certain way.

In the case where a system operates in a wide spectral range, there are no serious problems with optical elements used to focus light beams and form the necessary number of measurement channels. To eliminate the influence of chromatism, reflecting metal-coated elements operating at small (several degrees) angles of incidence and mirror beamsplitters are used. For angles of incidence as low as these, metal-coated mirror surfaces have no effect on the polarization state being measured [20].

Glan–Taylor prisms are commonly used for applications where an analyzer of linear polarization is required. This analyzer consists of two calcite prisms separated by an air gap and provides high transmission and a high degree of polarization [12]. In view of the fact that the prisms are not glued, the analyzer can operate in a spectral range determined only by the iceland spar transmittance (0.2–2.0 μm). Moreover, the production of such prisms requires the smallest amount of expensive iceland spar (calcite). However the use of Glan–Taylor prisms limits the operating angular aperture to a value of less than 7°.

In addition to Glan–Taylor prisms, other right-angled prisms are used as polarization analyzers [12, 26]: Glan prisms glued with optical cement (Glan–Thompson prisms), Glazenbrook prisms, Gartnake–Prazmovsky prisms, and Arense prisms. The use of optical cement increases the angular aperture to 30–40° but limits

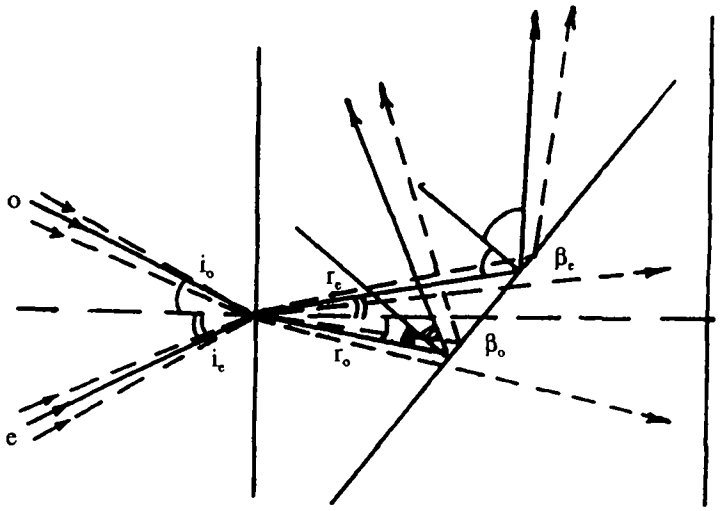

Fig. 1. Optical diagram illustrating the operation of the Glan–Taylor polarization prism.

the operating spectral range, increases the prism length by a factor of 3–4 and, consequently, increases the amount of expensive material required for prism fabrication.

Let us consider a Glan–Taylor prism with refraction angle α (Fig. 1). A light beam o incident on the prism face at angle i_o is propagated in the prism at angle r_o and is termed an ordinary beam. The angles are read from the normal to the interface. The relationship between the angles is described by a law of refraction with refractive index n_o for an ordinary beam. If this beam propagates within the limits of the operating angular aperture, it undergoes total internal reflection at the inner prism face. The condition of total internal reflection can be written in the form

$$\sin \beta_o \geq \frac{1}{n_o} , \tag{1}$$

where

$$\alpha - r_o = \beta_o . \tag{2}$$

Total internal reflection is not observed for $i > i_o$. The angle i_o limits the operating angular aperture on one side.

A light beam e incident on the prism at angle i_e and propagating inside the prism at angle r_e is an extraordinary beam. The relationship between these angles is given by a law of refraction with refractive index n_e for an extraordinary beam. This beam does not undergo total internal reflection at the inner prism face within the limits of the operating angular aperture. Total internal reflection is not observed for

$$\sin \beta_e \leq \frac{1}{n_e} , \tag{3}$$

where

$$\alpha + r_e = \beta_e . \tag{4}$$

Total internal reflection takes place for $i > i_e$. The angle i_e limits the operating angular aperture on the other side. The equality sign in expressions (1) and (3) corresponds to the operating angular aperture. The symmetric aperture angle is determined by the condition

$$i_o = i_e = i . \tag{5}$$

TABLE 1. Variation of Angles for Wavelength Ranges of 0.36–0.67 μm and 1.23–1.61 μm

Value	0.36–0.67 μm	1.23–1.61 μm
β_o	36.20°–37.21°	37.50°–37.77°
β_e	41.73°–42.35°	42.55°–42.62°
$r_o + r_e$	5.15°–5.54°	4.84°–4.96°
$2i$	8.05°–8.81°	7.51°–7.72°
α	38.80°–39.64°	39.94°–40.07°

Calculation based on the dependence of the refractive indices on the wavelength [28, 29] makes it possible to determine β_o and β_e [see (1) and (3)] and, therefore, r_o+r_e [see (2) and (4)], $2i = 2(\beta_e-\beta_o)n_on_e/(n_o+n_e)$ [see (5)], and α [see (2) and (4)]. The spectral range chosen for the calculation covers the visible region (0.36–0.67 μm) and the near-infrared region (1.23–1.61 μm), which are used in fiber communication lines. In the calculation, the values of sine functions may be set equal to the arguments for small angles. The results of the calculation for some wavelength ranges are presented in Table 1. One can see that the angular parameters vary only insignificanly over the spectral range under consideration.

In practice, the angle of refraction of the prism is chosen to have a minimum value $\alpha = \alpha_o$ for the operating spectral range. In this case, the reflection light losses have a minimum value and the amount of material required for prism production is minimal as well. But the operating aperture is slightly smaller under these conditions. Table 2 presents the results of calculations of the angles of incidence i_o and i_e, the refraction angles r_o and r_e [see (2) and (4)], the angular aperture $2i_{oe} = i_o + i_e$, and the angle ψ between the axis of the angular aperture and the prism axis, which is given by the relation

$$\psi = \frac{i_e - i_o}{2} .$$

The calculations were performed for a prism with refraction angle $\alpha_0 = 38.5°$ for the spectral ranges mentioned above. The results show that the chromatism of the Glan–Taylor prism has an insignificant effect. The angular aperture of the prism is equal to several degrees. The angle between the axis of the angular aperture and the prism axis is smaller than 2.5°.

Phase plates are elements which allow a polarization state to be changed without any change in optical intensity. Phase plates are commonly made of crystalline quartz. The phase shift $\delta(\lambda)$ produced by a plate with thickness h for radiation with wavelength λ is determined by the expression

$$\delta(\lambda) = \frac{2\pi h}{\lambda}[n_e(\lambda) - n_o(\lambda)] . \tag{6}$$

The phase shift $\delta(\lambda)$ depends on the wavelength and the material dispersion. To obtain the required phase difference of $\pi/2 + 2m\pi$, a phase plate must have thickness

$$h_m = \frac{(2m+1)\lambda}{4[n_e(\lambda) - n_o(\lambda)]} , \tag{7}$$

TABLE 2. Variation of Aperture Angles for Wavelength Ranges of 0.36–0.67 μm and 1.23–1.61 μm

Value	0.36–0.67 μm	1.23–1.61 μm
r_o	1.29°–2.30°	0.73°–0.91°
r_e	3.24°–3.85°	4.05°–4.12°
i_o	2.14°–3.90°	1.19°–1.50°
i_e	4.86°–5.72°	5.99°–6.08°
$i_o + i_e$	7.86°–8.75°	7.27°–7.49°
ψ	0.48°–1.79°	2.25°–2.45°

where m is the order of the plate. The thicknesses h_0 and h_1 for phase plates with orders $m = 0$ and $m = 1$ were calculated by formula (7) with the refractive indices taken from [28]. The calculations gave

$$9.15\ \mu\text{m} \le h_0 \le 19.63\ \mu\text{m}\ ,$$
$$27.45\ \mu\text{m} \le h_1 \le 58.88\ \mu\text{m}$$

for the visible region of the spectrum (0.36–0.70 μm) and

$$34.48\ \mu\text{m} \le h_0 \le 47.06\ \mu\text{m}\ ,$$
$$103.45\ \mu\text{m} \le h_1 \le 141.18\ \mu\text{m}$$

for the near-infrared region (1.20–1.60 μm). One can see that chromatism is of considerable importance for phase plates.

The effect of chromatism can be eliminated in two different ways. One is by the use a Babinet–Soleil compensator [12, 20] with computer-controlled thickness for a preset wavelength, which must be entered into the computer beforehand. Alternatively, one may take into account the wavelength dependence of the phase shift $\delta(\lambda)$ in the course of processing measurement results when a phase plate of constant thickness is used. The second method is preferable in practice. Consideration of the wavelength dependence is necessary in the case of measurements in a wide spectral range. Note that it is simpler and cheaper to fabricate a phase plate with constant thickness than a compensator with mechanical control.

Table 3 presents the results of calculations of phase shifts $\delta(\lambda)$ [see (6)] produced by phase plates of zero and first orders with a fixed thickness h. The refractive indices are taken from [28]. Moreover, the table presents the distributions $\Delta\delta(\lambda)$ of phase shift from $\pi/2$ for zero-order phase plates and from $3\pi/2$ for first-order phase plates. The plate thicknesses are such that the phase shift is about $\pi/2$ or, respectively, $3\pi/2$ for the centers of the given spectral ranges (0.36–0.50 μm, 0.40–0.70 μm, and 1.20–1.60 μm). The width of the spectral ranges is such that the deviations $\Delta\delta(\lambda)$ of the phase shifts from $\pi/2$ are approximately symmetric in each range and do not exceed 30 % for the zero-order plates.

These results show that the zero-order phase plate is preferable for operation in a wide spectral range. In contrast, first-order phase plates give poorer results. For the same deviations of phase shifts from $\pi/2$, they operate in narrower spectral ranges. We emphasize that the inclusion of phase shifts from $\pi/2$ in the consideration requires a special spectral study. These questions are considered below for a specific measuring system (see Sec. 2).

TABLE 3. Phase Shifts $\delta(\lambda)$ for Zero- and First-Order Phase Plates of Thickness h_0 and h_1 and Deviations $\Delta\delta(\lambda)$ of these Phase Shifts from $\pi/2$ and $3\pi/2$ for Zero- and First-Order Plates in the Visible and Near-Infrared Regions, Respectively

λ, nm	$h_0 = 11.0$ μm		14.0 μm		40.0 μm		$h_1 = 33.0$ μm		41.0 μm		120.0 μm	
	$\delta(\lambda)$	$\Delta\delta(\lambda)$	$\delta(\lambda)$	$\Delta\delta(\lambda)$	$\delta(\lambda)$	$\Delta\delta(\lambda)$	$\delta(\lambda)$	$\Delta\delta(\lambda)$	$\delta(\lambda)$	$\Delta\delta(\lambda)$	$\delta(\lambda)$	$\Delta\delta(\lambda)$
358.7	1.8883	0.3175					5.6648	0.9524				
404.7	1.6223	0.0516	2.0507	0.4799			4.8673	0.1549	6.0472	1.3348		
508.6	1.2638	−0.3070	1.6085	0.0377			3.7914	−0.9210	4.7105	0.0019		
589.3			1.3733	−0.1975					4.0218	−0.6906		
706.5			1.1206	−0.4502					3.2816	−1.4307		
1200.0					1.8251	0.2513					5.4664	0.7540
1300.0					1.6626	0.0918					4.9879	0.2755
1400.0					1.5439	−0.0269					4.6316	−0.0808
1529.6					1.3966	−0.1742					4.1899	−0.5225
1600.0					1.3352	−0.2356					4.0056	−0.7068

Note that the production of phase plates with a small thickness requires a special technology. One may use for this purpose an additional substrate made from an isotropic material such as fused quartz. Another method is to use two plates made from crystalline quartz with mutually orthogonal axes. The difference in the thickness of the two plates must be equal to the required value.

The operating angular aperture of a phase plate can be analyzed taking into account oblique incidence of beams on it (Fig. 2). For a ray that is incident on a plate of thickness h at angle i, the optical path length (inside the plate) is given by the expression

$$h' = \frac{h}{\cos r} \approx \frac{h}{1 - r^2/2},$$

where r is the refraction angle ($r \approx r_o, r_e$). Let the change Δh in the optical path (due to oblique incidence) be smaller than $0.001\,h$. Then, angle i must be smaller than the value determined by the condition

$$r_o,\ r_e < 0.04 \text{ rad} \qquad \text{or} \qquad i < n_o r_o,\ n_e r_e \approx 0.06 \text{ rad} \approx 3.5°.$$

For the given accuracy of phase shift measurement (about 0.001 rad), the influence of the angular aperture of a phase plate made of crystalline quartz may be neglected if it is smaller than 7°. Note that this value is very close to the angular aperture of the Glan–Taylor prism.

Note that a phase plate of a definite thickness may be used in the zero order in the long-wavelength region and in the first order in the short-wavelength region. In particular, this variant can be realized for a phase plate with thickness $h \approx 40.0$–41.0 μm.

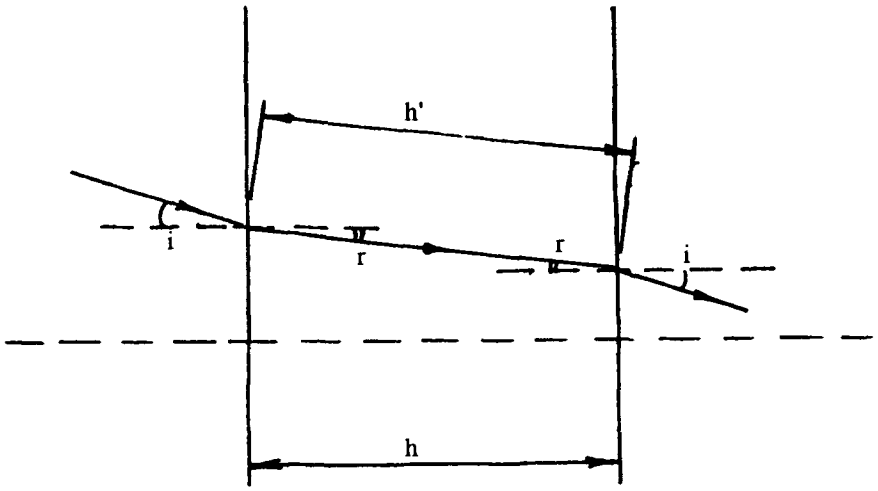

Fig. 2. Optical diagram for taking into account oblique incidence on a phase plate.

3. Four-Channel System for Measuring the Polarization of Laser Radiation

One of the main methods is the classical technique of measurement of optical intensity in four independent analyzing channels, each characterized by a specified polarization state [20, 21, 23]. In this section, we consider the operation of such a system and the methods by which the Stokes parameters can be experimentally determined [20, 21]. The Stokes parameters give a complete description of the polarization state of quasi-monochromatic partially polarized radiation.

The parameters of the elements (polarization devices, mirrors) comprising an optical system determine its overall layout. For the system under consideration, the calculation of chromatism and angular aperture is of considerable importance.

For definiteness, we shall use a laboratory coordinate system in which the x axis is directed horizontally and the y axis is directed vertically. Both axes are orthogonal to the direction of radiation propagation.

In the general case, quasi-monochromatic and partially polarized incident radiation under analysis can be decomposed into two components corresponding to natural and polarized light with intensities $I_{\text{nat}}(t)$ and $I_{\text{pol}}(t)$, respectively. The latter component may have linear, circular, elliptic, or mixed polarization. Irrespective of the polarization type, the polarized component may be represented in the laboratory coordinate system in the form of the fields [20, 21].

$$\begin{aligned} E_x(t) &= \mathcal{E}_x(t)\exp[-i\omega t + i\delta_x(t)] \; ; \\ E_y(t) &= \mathcal{E}_y(t)\exp[-i\omega t + i\delta_y(t)] \; ; \\ \delta(t) &= \delta_y(t) - \delta_x(t) \; . \end{aligned} \tag{8}$$

The time dependences of intensities $I_{\text{nat}}(t)$ and $I_{\text{pol}}(t)$, amplitudes $\mathcal{E}_x(t)$ and $\mathcal{E}_y(t)$, and phase shifts $\delta_x(t)$, $\delta_y(t)$, and $\delta(t)$ are related to the quasi-monochromaticity of the radiation being analyzed. The instantaneous intensity of the polarized component is given by the expression [see (8)]

$$I_{\text{pol}}(t) = I_{\text{pol}\,x}(t) + I_{\text{pol}\,y}(t) = \mathcal{E}_x^2(t) + \mathcal{E}_y^2(t) \; , \tag{9}$$

where $I_{\text{pol}\,x}(t)$ and $I_{\text{pol}\,y}(t)$ are the instantaneous intensities of the polarized components with electric field vectors directed along the x and y axes, respectively.

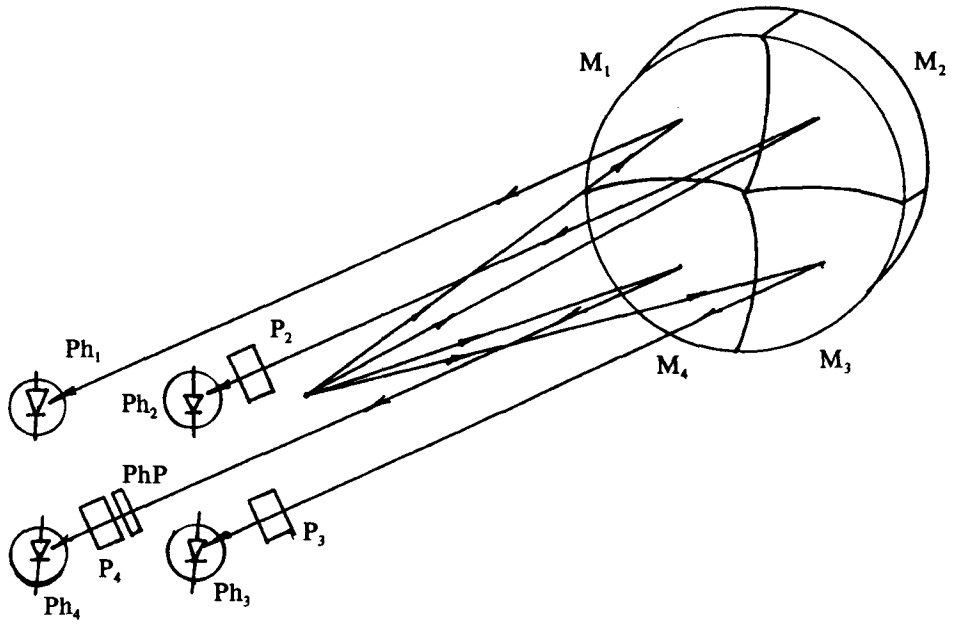

Fig. 3. Optical diagram of a four-channel polarization analyzer: M_1–M_4 are spherical sectional mirrors, P_2–P_4 are polarization prisms, PhP is a phase plate, and Ph_1–Ph_4 are photoelectric detectors.

In the case under consideration, the intensities of optical signals are measured in four channels. A schematic diagram of the system with four optical signals formed by four spherical mirrors M_1–M_4 is presented in Fig. 3. Let us determine the conditions required for measuring intensity by four photoelectric detectors Ph_1–Ph_4. It should be noted that in the general case, the amplitudes $\mathcal{E}_x(t)$ and $\mathcal{E}_y(t)$ and the phase shifts $\delta_x(t)$, $\delta_y(t)$, and $\delta(t)$ may change during the time Δt in which quasi-monochromatic radiation is measured. This means that the characteristic time for changes in the polarization state of radiation being analyzed or the radiation coherence time $t_{\text{coh}} \sim 1/\Delta\nu$ are smaller than the measurement time Δt. This allows one to write the time-averaged intensities in the form

$$\begin{aligned} I_{\text{pol } x} &= < \mathcal{E}_x^2(t) > ; \\ I_{\text{pol } y} &= < \mathcal{E}_y^2(t) > ; \\ I_{\text{pol } xy} &= < \mathcal{E}_x(t)\mathcal{E}_y(t) > . \end{aligned} \tag{10}$$

The situation is simplified when t_{coh} exceeds Δt. In this case, instantaneous intensities are measured and time averaging is of no importance.

For the generality of our further analysis, we shall take into account the inaccuracy of measurements as a function of the intensity error ΔI, the angle error for the installation of polarization elements $\Delta\vartheta$, and the error corresponding to phase shift induced by a phase plate $\Delta\delta(\lambda)$. The error analysis is performed in a conventional way using expansion in terms of a small parameter, a Gaussian distribution for random errors, and linearization of random errors by expansion in series [30].

The first channel measures the radiation intensity without any polarization elements. This measurement gives the intensity [see (9) and (10)]

$$I_0 = I_{\text{nat}} + I_{\text{pol}} = I_{\text{nat}} + < \mathcal{E}_x^2(t) > + < \mathcal{E}_y^2(t) > . \tag{11}$$

Note that in another version of the technique, the intensity in the first channel is measured with a polarization element which separates out linear polarization with orientation along one of the axes of the laboratory coordinate system. For example, it may be directed along the y axis. However, this requires an additional polarization prism, which may be inconvenient. In this work, such a system is not analyzed.

In the second channel, a polarizer P_2 specifying linear polarization along the x axis is placed before the photodiode Ph_2 and is used as an analyzer. In view of (9) and (10), measurement gives the intensity

$$I_x = I_{\text{nat}\,x} + I_{\text{pol}\,x} = \frac{I_{\text{nat}}}{2} + < \mathcal{E}_x^2(t) > , \tag{12}$$

where $I_{\text{nat}\,x}$ is the intensity of that component of nonpolarized radiation whose electric vector is directed along the x axis. It is evident that $I_{\text{nat}\,x} = I_{\text{nat}}/2$.

We emphasize that this polarizer is assumed to determine the position of the laboratory coordinate system. Because of this, errors of orientation of other polarization elements are estimated under the assumption that this element has an exact orientation.

In the third channel, an analyzer P_3 specifying linear polarization oriented at angle ϑ_1 to the x axis is used. It separates from the polarized component of incident light the signal [see (8) and Fig. 4]

$$E_{\text{pol}}^{\vartheta_1}(t) = E_x(t)\cos\vartheta_1 + E_y(t)\sin\vartheta_1 .$$

The radiation intensity measured in this way is described by the expression

$$\begin{aligned} I^{\vartheta_1} &= I_{\text{nat}}^{\vartheta_1} + I_{\text{pol}}^{\vartheta_1} = \frac{I_{\text{nat}}}{2} + < E_{\text{pol}}^{\vartheta_1}(t)\; E_{\text{pol}}^{\vartheta_1\,*}(t) > \\ &= \frac{I_{\text{nat}}}{2} + < \mathcal{E}_x^2(t) > \cos^2\vartheta_1 + < \mathcal{E}_y^2(t) > \sin^2\vartheta_1 + < \mathcal{E}_x(t)\mathcal{E}_y(t) > \sin 2\vartheta_1 \cos < -\delta(t) > . \end{aligned} \tag{13}$$

In the fourth channel, the radiation passes through the phase plate PhP producing an additional phase shift $\delta(\lambda)$. It is assumed that the phase plate has a constant thickness h (see Sec. 2). Its action on the phases of the field components oriented along the x and y axes are described by the quantities $\delta_x(t)$ and $\{\delta_y(t) - \delta(\lambda)\}$, respectively. In this channel, an analyzer P_4 is oriented at angle ϑ_2 to the x axis. The field $E_{\text{pol}}^{\vartheta_2}(t)$ separated from the polarized component of light (see Fig. 4) is given by the expression

$$E_{\text{pol}}^{\vartheta_2}(t) = E_x(t)\cos\vartheta_2 + E_y(t)\exp[-i\delta(\lambda)]\sin\vartheta_2 .$$

The intensity measured in the channel is described by the expression

$$\begin{aligned} I^{\vartheta_2} &= I_{\text{nat}}^{\vartheta_2} + I_{\text{pol}}^{\vartheta_2} = \frac{I_{\text{nat}}}{2} + < E_{\text{pol}}^{\vartheta_2}(t) E_{\text{pol}}^{\vartheta_2\,*}(t) > \\ &= \frac{I_{\text{nat}}}{2} + < \mathcal{E}_x^2(t) > \cos^2\vartheta_2 + < \mathcal{E}_y^2(t) > \sin^2\vartheta_2 + < \mathcal{E}_x(t)\mathcal{E}_y(t) > \sin 2\vartheta_2 \cos < [\delta(\lambda) - \delta(t)] > . \end{aligned} \tag{14}$$

Thus, the information recorded by the method contains the parameters $I_0, I_x, I^{\vartheta_1}$, and I^{ϑ_2} [see (11)–(14)].

In this case, the Stokes parameters are described by the expressions [20, 21]

$$\begin{aligned} S_0 &= I_{sx} + I_{sy} = I_0 ; \\ S_1 &= I_{sx} - I_{sy} ; \\ S_2 &= 2 < \mathcal{E}_x(t)\mathcal{E}_y(t) > \cos < [\delta_x(t) - \delta_y(y)] > ; \\ S_3 &= 2 < \mathcal{E}_x(t)\mathcal{E}_y(t) > \sin < [\delta_x(t) - \delta_y(y)] > , \end{aligned} \tag{15}$$

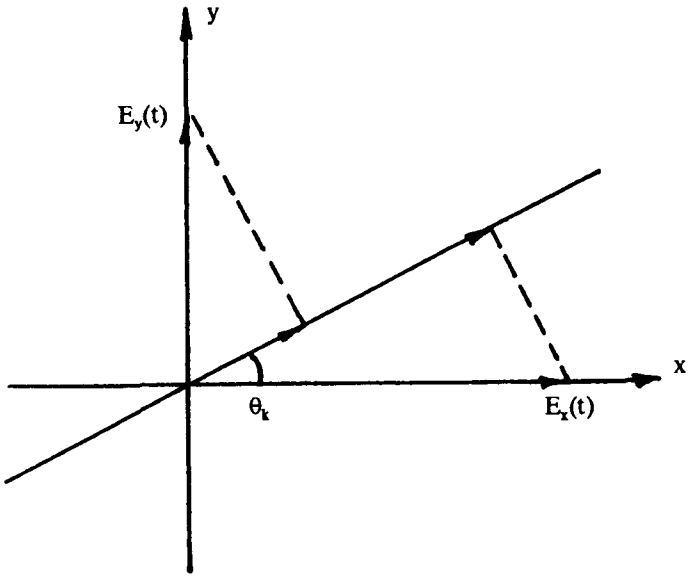

Fig. 4. Separation of a certain polarization of radiation; ϑ_k corresponds to ϑ_1 and ϑ_2 (see Sec. 3) or ϑ (see Sec. 4 or Sec 5).

and

$$\begin{aligned} I_{\text{pol}}^2 &= S_1^2 + S_2^2 + S_3^2 \, ; \\ I_{\text{nat}} &= I_0 - I_{\text{pol}} = S_0 - I_{\text{pol}} \, . \end{aligned}$$

The subscript s indicates the total intensity for the given polarization. The formulas for the system under consideration are given below.

The Stokes parameter S_0, in view of (11) and (15), has the form

$$S_0 = I_0 = I_{\text{nat}} + I_{\text{pol}} = I_{\text{nat}} + < \mathcal{E}_x^2(t) > + < \mathcal{E}_y^2(t) \, . \tag{16}$$

Taking into account the error ΔI for measurements of intensity I_0, we have

$$\Delta S_0 = \Delta I \, . \tag{17}$$

The Stokes parameter S_1, in view of (11), (12), and (15), is determined by the expression

$$S_1 = < \mathcal{E}_x^2(t) > - < \mathcal{E}_y^2(t) > = I_x - (I_0 - I_x) = 2I_x - I_0 \, . \tag{18}$$

Taking into account the errors ΔI for measurements of intensities I_0 and I_x, we have

$$\Delta S_1 = [(2\Delta I)^2 + (\Delta I)^2]^{1/2} = [5(\Delta I)^2]^{1/2} \, . \tag{19}$$

The Stokes parameter S_2, in view of (13) and (15), is determined by the expression

$$S_2 = \frac{2I^{\vartheta_1} - I_{\text{nat}} - 2 < \mathcal{E}_x^2(t) > \cos^2 \vartheta_1 - 2 < \mathcal{E}_y^2(t) > \sin^2 \vartheta_1}{\sin 2\vartheta_1} \, . \tag{20}$$

In the important case where measurements are carried out for $\vartheta_1 = \pi/4$, the previous expression can be simplified and has the form

$$S_2 = 2I^{\vartheta_1} - I_{\text{nat}} - < \mathcal{E}_x^2(t) > - < \mathcal{E}_y^2(t) >= 2I^{\vartheta_1} - I_0 \ . \tag{21}$$

Taking into account the errors ΔI for the intensities I_0 and I^{ϑ_1} and $\Delta\vartheta$ for the polarizer angle ϑ_1, we obtain, in view of (18) and (20), for the angle $\vartheta_1 = \pi/4$ the relation

$$\Delta S_2 = \left[(2\Delta I)^2 + (\Delta I)^2 + 4\left(< \mathcal{E}_x^2(t) > - < \mathcal{E}_y^2(t) >\right)^2 (\Delta\vartheta)^2\right]^{1/2} = [5(\Delta I)^2 + 4S_1^2(\Delta\vartheta)^2]^{1/2} \ . \tag{22}$$

The Stokes parameter S_3, in view of (15), is

$$S_3 = 2 < \mathcal{E}_x(t)\mathcal{E}_y(t) > \sin < [\delta_x(t) - \delta_y(t)] >$$

and

$$I^{\vartheta_2} = \frac{I_{\text{nat}}}{2} + < \mathcal{E}_x^2(t) > \cos^2\vartheta_2 + < \mathcal{E}_y^2(t) > \sin^2\vartheta_2 + \frac{S_2}{2}\sin 2\vartheta_2 \cos\delta(\lambda) - \frac{S_3}{2}\sin 2\vartheta_2 \sin\delta(\lambda) \ . \tag{23}$$

For measurements carried out for $\vartheta_2 = \pi/4$, we obtain, in view of (21) and (23),

$$I^{\vartheta_2} = \frac{I_0}{2} + \frac{S_2}{2}\cos\delta(\lambda) - \frac{S_3}{2}\sin\delta(\lambda) \ .$$

Finally, in view of (11), (20), and (23), we have

$$S_3 = \frac{-2I^{\vartheta_2} + I_0 + S_2\cos\delta(\lambda)}{\sin\delta(\lambda)} \ . \tag{24}$$

As before, we can find the error ΔS_3 associated with the errors ΔI for intensities I_0 and I^{ϑ_2}, the error $\Delta\vartheta$ for the polarizer angle ϑ_2, and the error of phase plate orientation. The latter error causes the error $\Delta\delta(\lambda)$ for the phase shift $\delta(\lambda)$. Taking into account expressions (18), (20), and (23) for S_1, S_2, and I^{ϑ_2}, calculation of ΔS_3 on the basis of (24) for $\vartheta_2 = \pi/4$ gives

$$\begin{aligned} \Delta S_3 &= \left[(2\Delta I)^2 + (\Delta I)^2 + 4(< \mathcal{E}_x^2(t) > - < \mathcal{E}_y^2(t) >)^2(\Delta\vartheta)^2 + \left(\frac{S_2}{\sin\delta(\lambda)}\right)^2 [\Delta\delta(\lambda)]^2\right]^{1/2} \frac{1}{\sin\delta(\lambda)} \\ &= \left[5(\Delta I)^2 + (2S_1)^2(\Delta\vartheta)^2 + \left(\frac{S_2}{\sin\delta(\lambda)}\right)^2 [\Delta\delta(\lambda)]^2\right]^{1/2} \frac{1}{\sin\delta(\lambda)} \ . \end{aligned} \tag{25}$$

For a phase plate of constant thickness h and a given wavelength λ, the phase shift $\delta(\lambda)$ [see (6)] and the Stokes parameter S_3 can be calculated using the known refractive indices $n_o(\lambda)$ and $n_e(\lambda)$. It should be noted that $\delta(\lambda)$ must not be a multiple of π or close to this value. The system considered above allows one to perform measurements over a wide spectral range by using several phase plates. It should be also noted that polarization prisms and phase plates operate with small errors only for angular apertures as low as few degrees (see Sec. 2). The fulfilment of this condition is provided by mirrors M_1–M_4 (see Fig. 3) or additional mirrors.

Let us note the simplest case corresponding to precise adjustment of the polarizers and the phase plate. In this case, we have

$$\Delta\vartheta = 0, \quad \Delta\delta(\lambda) = 0 \ .$$

This gives

$$\begin{aligned} S_0 &= I_0; \\ S_1 &= 2I_x - I_0; \\ S_2 &= 2I^{\vartheta_1} - I_0; \\ S_3 &= \frac{-2I^{\vartheta_2} + I_0 + S_2 \cos\delta(\lambda)}{\sin\delta(\lambda)} \end{aligned} \tag{26}$$

and

$$\begin{aligned} \Delta S_0 &= \Delta I; \\ \Delta S_1 &= [5(\Delta I)^2]^{1/2}; \\ \Delta S_2 &= [5(\Delta I)^2]^{1/2}; \\ \Delta S_3 &= \frac{[5(\Delta I)^2]^{1/2}}{\sin\delta(\lambda)} . \end{aligned} \tag{27}$$

These expressions are convenient for simplified quantitative estimates.

4. System with Electrooptic Phase Modulator for Measuring Maximum and Minimum Intensities

For measuring the polarization of partially polarized quasi-monochromatic radiation, several versions of modulating systems have been reported [22–25]. Here, we consider a scheme with an electrooptic modulator. This scheme makes it possible to increase the measurement rate with respect to the rate provided by mechanical modulators. Let us consider its operation and the technique of data processing used to obtain Stokes parameters.

As before (Sec. 3), the radiation under analysis consists of natural light with instantaneous intensity $I_{\text{nat}}(t)$ and completely polarized light with intensity $I_{\text{pol}}(t)$ [see (9)]. The field of the polarized component in the laboratory coordinate system is described by Eq. (8).

Figure 5 illustrates the basic scheme of the method. A mirror M_0 forms a light beam with low divergence that passes through an electrooptic modulator EOM. The output radiation is split by a double mirror M_1–M_2 and directed into channels 1 and 2. Polarizers P_1 and P_2 in these channels are used to separate out linearly polarized radiation with prescribed orientation. Radiation passing through polarizers P_1 and P_2 is detected by photodiodes Ph_1 and Ph_2.

A phase modulator based on an electrooptic cell EOM affects the polarized component [31]. The cell is oriented in accordance with the laboratory coordinate system. In other words, its orientation determines the position of the laboratory coordinate system. The influence of the phase modulator on the polarized component of radiation can be described by the expressions

$$\begin{aligned} \varphi_x(t) &= \frac{\omega}{c} l\, n_x(t) ; \\ \varphi_y(t) &= \frac{\omega}{c} l\, n_y(t) , \end{aligned} \tag{28}$$

where l is the cell thickness and $n_x(t)$, $n_y(t)$ are the time-dependent refractive indices corresponding to the x and y components of the field and affected by the modulator. The concrete form of expressions for $n_x(t)$ and $n_y(t)$ is determined by the modulator type, and is of no importance for the scheme under consideration.

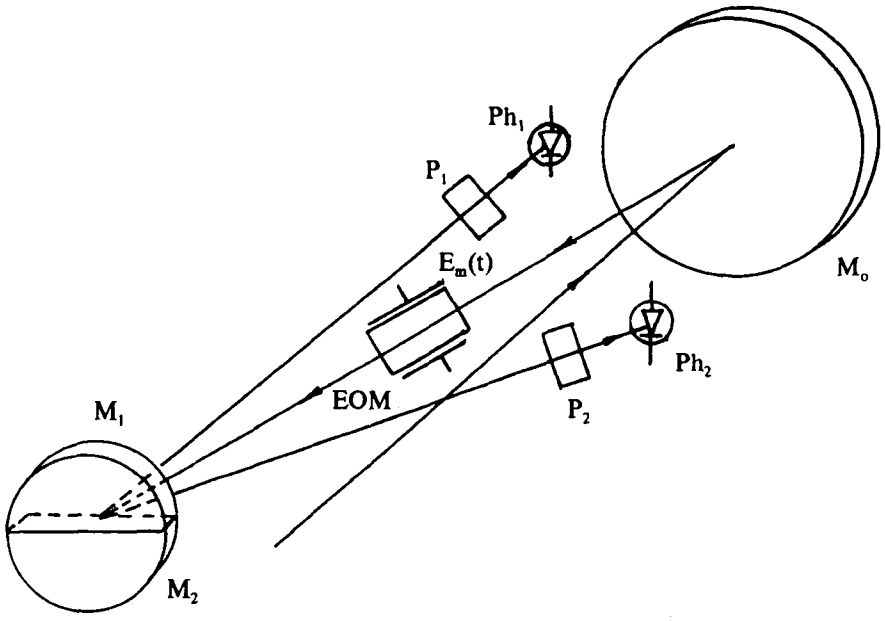

Fig. 5. Optical diagram of modulation polarization analyzer: M_0 is a focusing mirror; M_1 and M_2 are sectional focusing mirrors; EOM is an electrooptic phase modulator; P_1 and P_2 are polarization prisms; and Ph_1 and Ph_2 are photoelectric detectors.

As with the phase plate (see Sec. 3 and Fig. 2), the operating angular aperture of the electrooptic phase modulator can be determined taking into account the inclined path of rays through the cell. Let us assume that the relative change in the cell thickness for induced propagation is $\Delta h/h \approx 0.001$. This corresponds to forming the phase shift with an accuracy of 0.001 rad. In this case, the effect of the angular aperture on the operation of modulators with electrooptic crystals of the KDP type [31] (with a refractive index of about 1.5) is negligible for angles smaller than 7°. For electrooptic crystals of the niobate and tantalate type [31] (with a refractive index in a range of 2.0–2.5), the angle must not exceed 9°.

The polarized radiation at the output of the modulator has the form [see (8) and (28)]

$$\begin{aligned} E'_x(t) &= \mathcal{E}_x(t)\exp[-i\omega t + i\delta_x(t) + i\varphi_x(t)] \; ; \\ E'_y(t) &= \mathcal{E}_y(t)\exp[-i\omega t + i\delta_y(t) + i\varphi_y(t)] \; ; \\ \delta(t) &= \delta_y(t) - \delta_x(t) \; ; \\ \varphi(t) &= \varphi_y(t) - \varphi_x(t) \; . \end{aligned} \tag{29}$$

Further the radiation is directed to the output polarizer, which is oriented at angle ϑ with respect to the x axis (see Fig. 4). The polarized component of the radiation at the output of the polarizer has the form [see (29)]

$$E^{\vartheta}_{\text{pol}} = E'_x(t)\cos\vartheta + E'_y(t)\sin\vartheta \; . \tag{30}$$

The output intensity of the radiation is detected. The detection conditions associated with coherence of radiation and quasi-monochromaticity coincide with the conditions considered above for the four-channel scheme (see Sec. 3). The radiation must be modulated such that the characteristic time of changes in refractive indices $n_x(t)$ and $n_y(t)$ and, consequently, the time for changes in phase shifts $\varphi_x(t)$ and $\varphi_y(t)$

are greater than the characteristic detection time. In this case, the modulation of the interference component of radiation intensity is recorded.

The recorded intensity changes in time due to modulation and contains two components. The first component is associated with natural light partially passing through the polarizer. This component is not affected by the phase modulator and its intensity $I^{\vartheta}_{\text{nat}} = I_{\text{nat}}/2$. The second component corresponds to the polarized component of radiation separated by the polarizer [see (30)]

$$I^{\vartheta}_{\text{pol}}(t) = < E^{\vartheta}_{\text{pol}}(t)\, E^{\vartheta\,*}_{\text{pol}}(t) > \ .$$

As with (13), the total intensity is given by the expression [see (29) and (30)]

$$\begin{aligned} I^{\vartheta}(t) &= I^{\vartheta}_{\text{nat}} + I^{\vartheta}_{\text{pol}}(t) = \frac{I_{\text{nat}}}{2} + < E^{\vartheta}_{\text{pol}}(t)\, E^{\vartheta\,*}_{\text{pol}}(t) > \\ &= \frac{I_{\text{nat}}}{2} + < \mathcal{E}^2_x(t) > \cos^2\vartheta + < \mathcal{E}^2_y(t) > \sin^2\vartheta + < \mathcal{E}_x(t)\mathcal{E}_y(t) > \sin 2\vartheta \cos[< \delta(t) > + \varphi(t)] . \end{aligned} \tag{31}$$

The time dependence of intensity $I^{\vartheta}(t)$ is substantially affected by the phase modulation of $\varphi_x(t)$, $\varphi_y(t)$, and $\varphi(t)$ in time.

The system under consideration can be used to measure both the maximum and minimum intensities. Its operation is independent of the modulator type [20, 22]. However, the modulation depth must be considerable to ensure measurements of the maximum and minimum intensities.

The maximum intensity $I^{\vartheta}_{\text{max}}$ corresponds to the phase $\varphi(t) = \varphi_{\text{max}}$ defined by the expression [see (31)]

$$\cos[< \delta(t) > + \varphi_{\text{max}}] = 1 \qquad \text{or} \qquad < \delta(t) > + \varphi_{\text{max}} = 2m\pi \ , \tag{32}$$

and is equal to

$$I^{\vartheta}_{\text{max}} = \frac{I_{\text{nat}}}{2} + < \mathcal{E}^2_x(t) > \cos^2\vartheta + < \mathcal{E}^2_y(t) > \sin^2\vartheta + < \mathcal{E}_x(t)\mathcal{E}_y(t) > \sin 2\vartheta \ . \tag{33}$$

The minimum intensity $I^{\vartheta}_{\text{min}}$ corresponds to the phase $\varphi(t) = \varphi_{\text{min}}$ defined by the expression [see (31)]

$$\cos[< \delta(t) > + \varphi_{\text{min}}] = -1 \qquad \text{or} \qquad < \delta(t) > + \varphi_{\text{min}} = (2m+1)\pi \ , \tag{34}$$

and is equal to

$$I^{\vartheta}_{\text{min}} = \frac{I_{\text{nat}}}{2} + < \mathcal{E}^2_x(t) > \cos^2\vartheta + < \mathcal{E}^2_y(t) > \sin^2\vartheta - < \mathcal{E}_x(t)\mathcal{E}_y(t) > \sin 2\vartheta \ . \tag{35}$$

In these expressions m is an integer. In actuality it is equal to 0 or 1 .

To determine the Stokes parameters [see (15)], let us consider two combinations of the measured quantities $I^{\vartheta}_{\text{max}}$ and $I^{\vartheta}_{\text{min}}$. Taking into account (33) and (35), we have

$$I^{\vartheta}_{\text{max}} + I^{\vartheta}_{\text{min}} = S_0 + S_1(2\cos^2\vartheta - 1) \tag{36}$$

and

$$I^{\vartheta}_{\text{max}} - I^{\vartheta}_{\text{min}} = S_2 \frac{\sin 2\vartheta}{\cos < \delta(t) >} = S_3 \frac{\sin 2\vartheta}{\sin < \delta(t) >} \ . \tag{37}$$

For direct measurements carried out in one channel for a definite polarizer orientation (for example, for $\vartheta = \pi/4$), we have

$$\begin{aligned} I^{\pi/4}_{\text{max}} &= \frac{I_{\text{nat}}}{2} + \frac{< \mathcal{E}^2_x(t) >}{2} + \frac{< \mathcal{E}^2_y(t) >}{2} + < \mathcal{E}_x(t)\mathcal{E}_y(t) > \ ; \\ I^{\pi/4}_{\text{min}} &= \frac{I_{\text{nat}}}{2} + \frac{< \mathcal{E}^2_x(t) >}{2} + \frac{< \mathcal{E}^2_y(t) >}{2} - < \mathcal{E}_x(t)\mathcal{E}_y(t) > \ . \end{aligned}$$

In the expressions presented below, we will take into account the error ΔI associated with intensity measurements and the error $\Delta\vartheta$ associated with the angular orientation of the polarizer.

For $\vartheta = \pi/4$, in view of (36), the Stokes parameter S_0 is given by the expression

$$S_0 = I^{\vartheta}_{\max} + I^{\vartheta}_{\min} = I_{\text{nat}} + < \mathcal{E}^2_x(t) > + < \mathcal{E}^2_y(t) > . \tag{38}$$

Taking into account the errors ΔI and $\Delta\vartheta$, we can calculate ΔS_0 [see (36)]

$$\Delta S_0 = [2(\Delta I)^2 + 4S_1^2(\Delta\vartheta)^2]^{1/2} . \tag{39}$$

For $\vartheta = \pi/4$, in view of (37), the Stokes parameter S_2 is given by the expression

$$S_2 = (I^{\vartheta}_{\max} - I^{\vartheta}_{\min}) \cos < \delta(t) > . \tag{40}$$

Taking into account the errors ΔI, $\Delta\vartheta$, and $\Delta\varphi$, we calculate ΔS_2 [see (37) and (40)]

$$\Delta S_2 = [4\cos^2(2m\pi - \varphi_{\max})(\Delta I)^2 + (I^{\vartheta}_{\max} - I^{\vartheta}_{\min})^2 \sin^2(2m\pi - \varphi)(\Delta\varphi)^2]^{1/2} \tag{41}$$

for the polarizer angle $\vartheta = \pi/4$.

For $\vartheta = \pi/4$, in view of (37), the Stokes parameter S_3 is given by the expression

$$S_3 = (I^{\vartheta}_{\max} - I^{\vartheta}_{\min}) \sin < \delta(t) > . \tag{42}$$

Taking into account the errors ΔI, $\Delta\vartheta$, and $\Delta\varphi$, we calculate ΔS_3 [see (37) and (42)]

$$\Delta S_3 = [4\sin^2(2m\pi - \varphi_{\max})(\Delta I)^2 + (I^{\vartheta}_{\max} - I^{\vartheta}_{\min})^2 \cos^2(2m\pi - \varphi_{\max})(\Delta\varphi)^2]^{1/2} \tag{43}$$

for the polarizer angle $\theta = \pi/4$.

In these expressions, we set [see (32)]

$$< \delta(t) >= 2m\pi - \varphi_{\max} ,$$

but one may also use [see (34)]

$$< \delta(t) >= (2m + 1) - \varphi_{\min} .$$

To determine the Stokes parameter S_1, one should measure the intensity in the second channel, say, the intensity in the case where the polarizer is oriented along the x axis ($\vartheta = 0$). This gives [see (33), (35)]

$$I^0_{\max} = I^0_{\min} = I^0_x = \frac{I_{\text{nat}}}{2} + < \mathcal{E}^2_x(t) > . \tag{44}$$

As a result, the Stokes parameter S_1 is given by the expression [see (36), (37), and (44)]

$$\begin{aligned} S_1 &= (I^0_{\max} + I^0_{\min}) - (I^{\pi/4}_{\max} - I^{\pi/4}_{\min}) \\ &= [I_{\text{nat}} + < \mathcal{E}^2_x(t) >] - [I_{\text{nat}} + < \mathcal{E}^2_x(t) > + < \mathcal{E}^2_x(t) >] \\ &= < \mathcal{E}^2_x(t) > - < \mathcal{E}^2_y(t) > . \end{aligned} \tag{45}$$

Taking into account the error, we obtain as with (39)

$$\Delta S_1 = [2(\Delta I)^2 + 2(\Delta I)^2 + 4S_1^2(\Delta\vartheta)^2]^{1/2} = 2[(\Delta I)^2 + S_1^2(\Delta\vartheta)^2]^{1/2} . \tag{46}$$

The measuring system described above has some advantages. It has only two measurement channels and a small number of polarization elements: two polarizers and an electrooptic phase modulator. But it is

necessary to measure the maximum and minimum intensities and the corresponding phase shifts in one of the channels. In view of the high level of achromatism of Glan–Taylor polarization prisms and the simplicity of taking into account the phase shift for the chosen wavelength, one can carry out measurements in a wide spectral range. The difficulties connected with forming a high voltage (U is about 10–20 kV) for controlling the modulator can easily be solved due to the low power consumption and high operating frequency of the power supply (about 10 kHz).

The drawback of the method described above is the requirement that the values $I_{\max}^{\pi/4}$ and $I_{\min}^{\pi/4}$ be recorded one after another. This restricts the scheme to measurement where changes in the polarization state are slower than the modulation rate.

5. System with Electrooptic Modulator and Intensity Measurements at Different Modulation Harmonics

In this section, we consider another version of the system using an electrooptic modulator for measuring the polarization of a partially polarized quasi-monochromatic beam. Sinusoidal phase modulation is used in the system. The intensity is measured in two channels by analyzing different orientations of linear polarization. This leads to detecting intensity modulation at harmonic frequencies, which provides information for determining the polarization state.

The optical scheme of this modification of the polarization analyzer is similiar to the one shown in Fig. 5. It contains the mirror M_0 forming a light beam in the electrooptic modulator EOM and the two-section mirror M_1–M_2 directing the light beams into the channels containing the polarizers P_1 and P_2 and the photoelectric detectors Ph_1 and Ph_2.

The general description of the modulator operation and the selection of a definite linear polarization is similar to that described in Sec. 4.

The polarized radiation being analyzed contains a component of natural light with intensity $I_{\text{nat}}(t)$ and a component of totally polarized light with intensity $I_{\text{pol}}(t)$. The field of the polarized component in the laboratory coordinate system is described by expressions (8) (see Sec. 3). The electrooptic phase modulator EOM determing the orientation of the laboratory coordinate system forms phase influences $\varphi_x(t)$ and $\varphi_y(t)$ on the field components $E_x(t)$ and $E_y(t)$, which are described by expressions (28) (see Sec. 4). The polarization field components at the modulator output have the form of (29). These fields are directed to the polarizer P_1 or P_2, which is oriented at angle ϑ to the x axis (see Fig. 4). At the polarizer output, the polarization field component $E_{\text{pol}}^{\vartheta}(t)$ has the form of (30). The detection conditions related to the quasi-monochromaticity and coherence of radiation are the same as those considered above for the four-channel system (see Sec. 3). Finally, the detected intensity

$$I^{\vartheta}(t) = I_{\text{nat}}^{\vartheta} + I_{\text{pol}}^{\vartheta}(t)$$

is described by expression (31).

In this variant of the system, one should specify the type of modulation. We shall consider a modulator based on the linear electrooptical Pockels effect. The control electric field $E_m(t)$ induces in the electrooptic crystal different changes in the refractive indices for the waves polarized along the x and y axes. The corresponding refractive indices are described by the formulas [31]

$$\begin{aligned} n_x(t) &= n_{ox} - rn_o^3\frac{E_m(t)}{2}\ ; \\ n_y(t) &= n_{ey} + rn_o^3\frac{E_m(t)}{2}\ , \end{aligned} \tag{47}$$

where n_{ox} and n_{ey} are the initial refractive indices of the material in a zero field and r is the electrooptic coefficient, which depends on the crystal used and its orientation. The time-dependent phase effect of the modulator on the light has the form [see (28), (31), and (47)]

$$\varphi(t) = \varphi_y(t) - \varphi_x(t) = \frac{\omega l}{c}[(n_{ey} - n_{ox}) + r n_o^3 E_m(t)] .$$

Let the modulator be driven by a sinusoidal electric field with amplitude E_m and frequency Ω

$$E_m(t) = E_m \sin \Omega t . \tag{48}$$

For the sake of simplicity, we introduce the notation

$$\begin{aligned} \varphi_{eo} &= \frac{\omega l}{c}(n_{ey} - n_{ox}) ; \\ \Phi_m &= \frac{\omega l}{c} r n_o^3 E_m ; \\ \varphi_m(t) &= \Phi_m \sin \Omega t . \end{aligned} \tag{49}$$

The constant phase factor φ_{eo}, caused by a birefringent material as described above or formed by a constant electric field, makes it possible to realize a quasi-linear regime. This regime is realized under the condition $\varphi_{eo} = \pi/2$ [31] (see Fig. 6). In view of (48) and (49), the expression for the modulated component of the detected intensity can be represented in the form [see (31)]

$$I_m^{\vartheta}(t) = < \mathcal{E}_x(t)\mathcal{E}_y(t) > \sin 2\vartheta \sin[< \delta(t) > + \Phi_m \sin \Omega t] . \tag{50}$$

Using trigonometric transformation of the factor $\sin[< \delta(t) > + \Phi_m \sin \Omega t]$ [32] we obtain the final expression for the detected intensity

$$\begin{aligned} I^{\vartheta}(t) &= \frac{I_{\text{nat}}}{2} + < \mathcal{E}_x^2(t) > \cos^2 \vartheta + < \mathcal{E}_y^2(t) > \sin^2 \vartheta \\ &- < \mathcal{E}_x(t)\mathcal{E}_y(t) > \sin(2\vartheta)\ J_0(\Phi_m)\ \sin < \delta(t) > \\ &- < \mathcal{E}_x(t)\mathcal{E}_y(t) > \sin(2\vartheta)\ 2J_1(\Phi_m)\ \cos < \delta(t) > \sin \Omega t \\ &- < \mathcal{E}_x(t)\mathcal{E}_y(t) > \sin(2\vartheta)\ 2J_2(\Phi_m)\ \sin < \delta(t) > \cos 2\Omega t \\ &- < \mathcal{E}_x(t)\mathcal{E}_y(t) > \sin(2\vartheta)\ 2J_3 1(\Phi_m)\ \cos < \delta(t) > \sin 3\Omega t \\ &- < \mathcal{E}_x(t)\mathcal{E}_y(t) > \sin(2\vartheta)\ 2J_4(\Phi_m)\ \sin < \delta(t) > \cos 4\Omega t \\ &- \cdots . \end{aligned} \tag{51}$$

Let us analyze the conditions for measuring the intensity $I^{\vartheta}(t)$ [see (51)] which make it possible to calculate the Stokes parameters S_0, S_1, S_2, S_3 [see (15)].

One can see from (51) that for any ϑ different from zero or $\pi/2$, the amplitude of the first harmonic of this intensity is related to the Stokes parameter S_2

$$I_{m\,\Omega}^{\vartheta} = < \mathcal{E}_x(t)\mathcal{E}_y(t) > \sin(2\vartheta)\ J_1(\Phi_m)\ \cos < \delta(t) > = S_2\ J_1(\Phi_m)\ \sin 2\vartheta$$

and

$$S_2 = \frac{I_{m\,\Omega}^{\vartheta}}{J_1(\Phi_m)\ \sin 2\vartheta} . \tag{52}$$

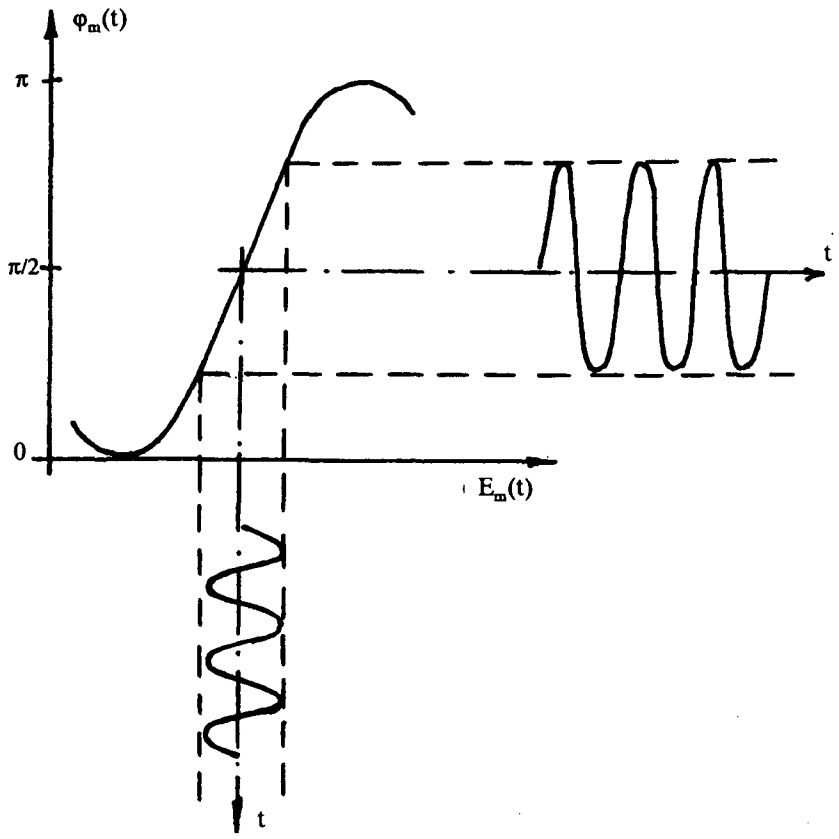

Fig. 6. Scheme illustrating the operation of the electrooptical Pockels modulator.

Calculation of the error ΔS_2 taking into account the errors ΔI and $\Delta\vartheta$ for measuring the intensity $I^{\vartheta}_{m\,\Omega}$ and setting the polarizer at angle ϑ gives

$$\Delta S_2 = \left\{(\Delta I)^2 + \left[2I^{\vartheta}_{m\,\Omega}\,\frac{\cos 2\vartheta}{\sin 2\vartheta}\right]^2 (\Delta\vartheta)^2\right\}^{1/2} \frac{1}{J_1(\Phi_m)\,\sin 2\vartheta}\,. \tag{53}$$

Note that the third-harmonic amplitude of the intensity of modulated radiation can also be used for determining the parameter S_2,.

In a similar way, from (51) for any ϑ follows the relationship between the second-harmonic amplitude and the Stokes parameter S_3

$$I^{\vartheta}_{m\,2\Omega} = <\mathcal{E}_x(t)\mathcal{E}_y(t)>\sin(2\vartheta)\,J_2(\Phi_m)\,\sin<\delta(t)> = S_3\,J_2(\Phi_m)\,\sin 2\vartheta$$

and

$$S_3 = \frac{I^{\vartheta}_{m\,2\Omega}}{J_2(\Phi_m)\,\sin 2\vartheta}\,. \tag{54}$$

Calculation of the error ΔS_3 taking into account the errors ΔI and $\Delta\vartheta$ in a way similar to that used for obtaining (53) gives

$$\Delta S_3 = \left\{(\Delta I)^2 + \left[2I^{\vartheta}_{m\,2\Omega}\,\frac{\cos 2\vartheta}{\sin 2\vartheta}\right]^2 (\Delta\vartheta)^2\right\}^{1/2} \frac{1}{J_2(\Phi_m)\,\sin 2\vartheta}\,. \tag{55}$$

The fourth-harmonic amplitude of the intensity of modulated radiation can be used for determining the parameter S_3.

In order to determine the other Stokes parameters, let us consider the zeroth harmonic $I^{\vartheta}_{m\ 0}$ of intensity for an arbitrary angle ϑ of polarizer orientation

$$I^{\vartheta}_{m\ 0} = \frac{S'_0}{2} - \frac{S_3}{2} J_0(\Phi_m) \sin 2\vartheta \ . \tag{56}$$

This gives

$$S'_0 = 2I^{\vartheta}_{m\ 0} + S_3 J_0(\Phi_m) \sin 2\vartheta \ . \tag{57}$$

As with the previous calculations, taking into account ΔS_3 [see (55)] the error $\Delta S'_0$ can be transformed into

$$\Delta S'_0 = \left\{ 4(\Delta I)^2 + \left[\frac{J_0(\Phi_m)}{J_2(\Phi_m)}\right]^2 (\Delta I)^2 + 4\cos^2 2\vartheta \left[\frac{I^{\vartheta}_{m\ 2\Omega}}{\sin 2\vartheta}\right]^2 (\Delta\vartheta)^2 + 4\cos^2 2\vartheta [S_3 J_0(\Phi_m)]^2 (\Delta\vartheta)^2 \right\}^{1/2} . \tag{58}$$

As mentioned above, the scheme under consideration has two measuring channels, each with a definite polarizer orientation. Let the polarizer orientation in the first channel be determined by the angle $\vartheta = \pi/4$ with respect to the x axis. One can measure the intensities of the zeroth, first and second harmonics $I^{\pi/4}_{m\ 0}$, $I^{\pi/4}_{m\ \Omega}$, $I^{\pi/4}_{m\ 2\Omega}$ using electrical filtering of harmonics. In the second channel, one measures the intensities $I^{0}_{m\ 0}$ or $I^{\pi/2}_{m\ 0}$ of the zeroth harmonics when the polarizer is oriented at the angle $\vartheta = 0$ or $\vartheta = \pi/2$ with respect to the x axis. For $\vartheta = \pi/4$, in view of (57), one can determine the Stokes parameter S_0 . Indeed,

$$I^{\pi/4}_{m\ 0} = \frac{S_0}{2} - \frac{S_3}{2} J(\Phi_m)$$

and, taking into account (54), we obtain

$$S_0 = 2I^{\pi/4}_{m\ 0} + \frac{S_3}{2} J_0(\Phi_m) \ . \tag{59}$$

In view of (58), the error ΔS_0 is given by the expression

$$\Delta S_0 = \left\{ 4 + \left[\frac{J_0(\Phi_m)}{J_2(\Phi_m)}\right]^2 \right\}^{1/2} \Delta I \ . \tag{60}$$

Using (57) and taking into account the intensity $I^{0}_{m\ 0}$ measured in the second channel with the polarizer oriented at the angle $\vartheta = 0$ with respect to the x axis, we have

$$I^{0}_{m\ 0} = \frac{I_{\rm nat}}{2} + < \mathcal{E}^2_x(t) > \ .$$

As a result

$$I^{\pi/4}_{m\ 0} - I^{0}_{m\ 0} = \frac{S_1}{2} + \frac{S_3}{2} J_0(\Phi_m) \ ,$$

which gives the Stokes parameter S_1

$$S_1 = 2(I^{0}_{m\ 0} - I^{\pi/4}_{m\ 0}) - S_3 J_0(\Phi_m) = 2I^{0}_{m\ 0} - S_0 \ . \tag{61}$$

In view of (60), the error ΔS_1 is given by the expression

$$\Delta S_1 = [(2\Delta I)^2 + (\Delta S_0)^2]^{1/2} = \left[\delta + \left(\frac{J_0(\Phi_m)}{J_2(\Phi_m)}\right)^2\right]^{1/2} \Delta I \ . \tag{62}$$

It is also possible to measure the intensity of the first harmonic for $\vartheta = \pi/2$. This gives the expressions

$$I_{m\,0}^{\pi/2} = \frac{I_{\text{nat}}}{2} + < \mathcal{E}_y^2(t) >$$

and

$$I_{m\,0}^{\pi/4} - I_{m\,0}^{\pi/2} = \frac{S_1}{2} - \frac{S_3}{2} J_0(\Phi_m) .$$

The Stokes parameter S_1 is determined by the formula

$$S_1 = 2(I_{m\,0}^{\pi/4} - I_{m\,0}^{\pi/2}) + S_3 J_0(\Phi_m) = S_0 - 2I_{m\,0}^{\pi/2} . \tag{63}$$

The estimate of the error ΔS_1 coincides with (62).

In view of (52), measurements of the amplitude of first harmonic in the first channel for $\vartheta = \pi/4$ give the expression for the Stokes parameter S_2

$$S_2 = \frac{I_{m\,\Omega}^{\pi/4}}{J_1(\Phi_m) \sin 2\vartheta} , \tag{64}$$

and [see (55)]

$$\Delta S_2 = \frac{1}{J_1(\Phi_m)} \Delta I . \tag{65}$$

Finally in view of (54), measurements of the second-harmonic amplitude in the first channel for the angle $\vartheta = \pi/4$ give the Stokes parameter S_3

$$S_3 = \frac{I_{m\,2\Omega}^{\pi/4}}{J_2(\Phi_m) \sin 2\vartheta} \tag{66}$$

and [see (55)]

$$\Delta S_3 = \frac{1}{J_2(\Phi_m)} \Delta I . \tag{67}$$

Thus, the intensities $I_{m\,0}^{\pi/4}$, $I_{m\,\Omega}^{\pi/4}$, $I_{m\,2\Omega}^{\vartheta}$ and $I_{m\,0}^{0}$ or $I_{m\,0}^{\pi/2}$ measured in two channels can be used to determine the Stokes parameters [see (59), (61) or (63), (64) and (66)]. The errors are determined by expressions (60), (62), (65), and (67).

In contrast to the method considered in Sec. 4, the system described here detects all the quantities simultaneously, i.e., one can measure the polarization of time-varying signals. These measurements allow one to determine the polarization state at any specified moment.

6. Conclusion

In conclusion, let us compare some characteristics of the three systems of polarization analizers considered above.

The operating spectral range of the systems under study is determined by the operating range of polarization elements, mainly of the polarization prisms. Polarization prisms made of iceland spar (calcite) with an air gap are used in the spectral range of 0.2–2.0 μm [12, 26]. Some limitations arise for polarization prisms with optical cement, because the latter has limited transmittance. As a rule, phase elements have a rather wide operating spectral range. The crystalline quartz used for phase plates (see Sec. 3) works well in the spectral range of 0.2–2.0 μm [12, 26]. Niobates and tantalates used for phase modulators (see Secs. 4 and 5) are transparent in the range of about 0.4–4.0 μm [31]. Electrooptic crystals of the KDP type [31] have a narrower spectral range (0.4–1.4 μm).

The operating angular aperture of the systems under consideration is limited by the polarization elements, which produce certain changes in the polarization state (phase plates or electrooptic phase modulators). For a deviation of phase influences set below 0.001 rad (see Sec. 3), the angular aperture of these elements is a few degrees. This value is typical for Glan–Taylor polarization prisms. The use of polarization prisms with a larger angular aperture (different types of polarization prisms with optical cement) does not have any effect in the systems under consideration.

A comparison of the possibilities for data recording and processing is also of interest.

It is clear that the four-channel system (see Sec. 3) requires four separate optical channels and four receivers. The recording system may be based on sequential interrogation of receptors. It is natural that this requires a noticeable increase in recording time. Such a system can be used for optical signals slowly varying in time. Rapidly varying signals require simultaneous recording with four parallel inputs and simultaneous signal storage. Some difficulties are caused by the need for reasonable accuracy of results obtained for the Stokes parameters. This is due to the fact that the Stokes parameters S_1, S_2, and S_3 are determined in the present case as differences between certain quantities [see expressions (18), (21), and (24)]. This requires a sufficiently high measurment accuracy. In particular, the use of 10-bit input registers ensures measurments of signals in separate channels within an accuracy of 0.1%. In view of the forming of differential quantities, this calls for an increased number of bits.

The modulation system with measurement of maximum and minimum intensities makes it possible to detect signals in two channels only (see Sec. 4). The characteristic feature of the system is the successive recording of maximum $I^{\vartheta}_{\max}$ and minimum $I^{\vartheta}_{\min}$ intensities. It is natural that the system can be used for optical signals with sufficiently slow temporal changes. The requirements on the measurment accuracy of this system are determined by the factors previously taken into account for the four-channel system. This is due to the fact that the determination of Stokes parameters S_1, S_2, and S_3 requires the values of signal differences [see expressions (40), (42), and (45)] to be used.

The modulation system with intensity measurements at different modulation harmonics also makes it possible to detect signals only in two channels (see Sec. 5). The characteristic feature is the need to separate signals at the modulation frequency and its harmonic frequencies during further processing. This calls for measurement of temporal variations of signals and further separation of harmonics, which increases the measurement time. However, these limitations may be greatly weakened for the case of high-frequency modulation and a high speed of signal recording. In this case, one must form a difference value only to determine the Stokes parameter S_1 [see (61)]. The other Stokes parameters are determined directly from the signal measurements. This makes it possible to lower the requirements on the accuracy of direct measurements.

References

1. H. G. Heard, *Laser Parameter Measurements, Handbook*, Wiley, New York (1968).
2. R. A. Valitov, N. G. Kokodii, A. V. Kubarev, et al., *Measurement of Laser Characteristics* [in Russian], Goskomstandart, Moscow (1969).
3. V. A. Zubov, *Methods for Measuring Laser Radiation Characteristics* [in Russian], Nauka, Moscow (1973).
4. *Abstracts of the Scientific and Technical Workshop on Phase and Polarization Measurements of Laser Radiation and their Metrological Support* [in Russian], VNIIOFI, Moscow (1978).
5. V. M. Stepanov (Ed.), *Phase and Polarization Measurements of Laser Radiation and their Metrological Support, Scientific Proceedings of the VNIIFTRI* [in Russian], Moscow (1981).
6. Yu. A. Ananiev, *Optical Resonators and the Problem of Laser Radiation Divergence* [in Russian], Nauka, Moscow (1979).

7. E. F. Ischenko, *Open Optical Resonators* [in Russian], Radio i Svyaz', Moscow (1980).
8. N. V. Karlov, *Lectures on Quantum Electronics* [in Russian], Nauka, Moscow (1983).
9. A. P. Voytovich and V. N. Severikov, *Lasers with Anisotropic Resonators* [in Russian], Nauka i Tekhnika, Minsk (1988).
10. A. M. Prokhorov (Ed.), *Handbook of Lasers* [in Russian], Sov. Radio, Moscow (1978), Vols. 1, 2.
11. W. Brunner and K. Junge, *Wissensspeicher Lasertekhnik*, VEB Fachbuchverlag, Leipzig (1987).
12. W. A. Shurkliff, *Polarized Light: Production and Use*, Harvard University Press, Cambridge (1962).
13. E. A. Volkova, *Polarization Measurements* [in Russian], Goskomstandart, Moscow (1974).
14. M. M. Gorshkov, *Ellipsometry* [in Russian], Sov. Radio, Moscow (1974).
15. N. D. Zhevandrov, *Application of Polarized Light* [in Russian], Nauka, Moscow (1978).
16. A. V. Rzhanov, K. K. Svitashev, A. I. Semenko, et al., *Foundations of Elipsometry* [in Russian], Nauka, Novosibirsk (1979).
17. R. M. A. Azzam and N. M. Bashara, *Ellipsometry and Polarized Light*, North–Holland, Amsterdam (1977).
18. V. K. Gromov, *Introduction to Ellipsometry* [in Russian], Leningrad State University, Leningrad (1986).
19. R. Cross, B. Heffner, and P. Hernday, "Polarization measurement goes automatic," *Laser and Optronics*, 25 (November 1991).
20. M. Born and E. Wolf, *Principles of Optics*, Pergamon Press, Oxford (1965).
21. F. S. Grawford, *Waves*, Berkley Physics Course, McGraw-Hill, New York (1969), Vol. 3.
22. B. M. Alentsev, M. Ya. Varshavskii, A. L. Veshchikov, et al., *Measurement of Frequency-Spectral and Correlation Parameters and Characteristics of Laser Radiation* [in Russian], Radio i Svyaz', Moscow (1982).
23. E. L. O'Neill, *Introduction to Statistical Optics*, Addison-Wesley Publ., Reading, MA (1963).
24. Yu. G. Vainer and U. V. Changildin, " Device for polarization investigation, " *Opt. Spektrosk.*, 41, 315 (1976).
25. *RPA 2000: The Complete Polarization Analyzer*, Instrument Systems Optische Messtekhnik GMBH, Munich, Germany.
26. D. V. Sivukhin, *General Physics: Optics* [in Russian], Nauka, Moscow (1965), Vol. 4.
27. G. S. Landsberg, *Optics* [in Russian], Nauka, Moscow (1976).
28. I. K. Kikoin (ed.), *Tables of Physical Quantities, Handbook* [in Russian], Atomizdat, Moscow (1976).
29. E. M. Voronkova, B. N. Grechushnikov, G. I. Distler, and I. P. Petrov, *Optical Materials for Infrared Instruments: Reference Book* [in Russian], Nauka, Moscow (1965).
30. A. A. Sveshnikov, *Foundations of Error Theory* [in Russian], Leningrad State University, Leningrad (1986).
31. E. R. Mustel' and V. N. Parygin, *Methods of Modulation and Scanning of Light* [in Russian], Nauka, Moscow (1970).
32. A. N. Tikhonov and A. A. Samarsky, *Equations of Mathematical Physics* [in Russian], Nauka, Moscow (1977).